Magnetic phase transition in half-metallic CoMnSb and NiMnSb semi-Heusler alloys upon Cu doping: First-principles calculations

I. Galanakis*
Department of Materials Science, School of Natural Sciences, University of Patras, GR-26504 Patra, Greece

E. Şaşıoğlu†
Institut für Festkörperforschung, Forschungszentrum Jülich, D-52425 Jülich, Germany
and Department of Physics, Fatih University, TR-34500 Büyükçekmece, İstanbul, Turkey

K. Özdoğan‡
Department of Physics, Gebze Institute of Technology, Gebze TR-41400, Kocaeli, Turkey
(Received 17 March 2008; revised manuscript received 30 April 2008; published 11 June 2008)

We study the effect of the nonmagnetic 3*d* atoms on the magnetic properties of the half-metallic (HM) semi-Heusler alloys $Co_{1-x}Cu_xMnSb$ and $Ni_{1-x}Cu_xMnSb$ ($0 \leq x \leq 1$) using first-principles calculations. We determine the magnetic phase diagram of both systems at zero temperature and obtain a phase transition from a ferromagnetic to an antiferromagnetic state. For low Cu concentrations the ferromagnetic Ruderman-Kittel-Kasuya-Yosida (RKKY)-type exchange mechanism dominates, while the antiferromagnetic superexchange coupling becomes important for larger Cu content. A strong dependence of the magnetism in both systems on the position of the Fermi level within the HM gap is found. Obtained results are in good agreement with the available experimental data.

DOI: 10.1103/PhysRevB.77.214417 PACS number(s): 75.50.Cc, 75.30.Et, 71.15.Mb

I. INTRODUCTION

In half-metallic semi-Heusler alloys with the chemical formula *X*Mn*Z*, where *X* is a high-valent transition metal atom and *Z* is an *sp* element, the magnetization is usually confined to the Mn sublattice and the total magnetic moment assumes integer values given by the Slater-Pauling rule.[1] Additionally, the Mn-Mn distance is rather large and thus the 3*d* states belonging to different Mn atoms do not overlap considerably. The ferromagnetism of the Mn moments stems from an indirect exchange interaction mediated by the conduction electrons. Therefore, the magnetic properties of these systems strongly depend on the nonmagnetic 3*d* (*X*) and *sp* (*Z*) atoms. Early measurements by Webster and Ziebeck[2] on several quaternary Heusler alloys as well as recent studies of Walle *et al.*[3] on $AuMnSn_{1-x}Sb_x$ demonstrated the importance of the *sp* electrons in establishing the magnetic properties. On the other hand, the importance of the nonmagnetic 3*d* atoms for the magnetism of Heusler alloys was revealed recently by the experimental studies of Duong *et al.*[4] and Ren *et al.*[5] The authors showed the possibility of tuning the Curie temperature of $Co_{1-x}Cu_xMnSb$ and $Ni_{1-x}Cu_xMnSb$ alloys by the substitution of Cu for Co and Ni, respectively. Furthermore, a phase transition from a ferromagnetic to an antiferromagnetic state is detected in both systems close to the stoichiometric composition ($x \sim 1$). We have to note here that CuMnSb is a well-known antiferromagnet and has been extensively studied both experimentally[6] and theoretically.[7]

The purpose of the given work is to investigate the influence of the nonmagnetic 3*d* atoms on the magnetic properties of the half-metallic semi-Heusler alloys $Co_{1-x}Cu_xMnSb$ and $Ni_{1-x}Cu_xMnSb$. We determine the magnetic phase diagram of both systems at zero temperature. In agreement with the experiments, we obtain a phase transition from a ferromagnetic to an antiferromagnetic state around $x \simeq 0.8$ and $x \simeq 0.6$ for the Co-based and Ni-based systems, respectively. The physical mechanisms behind the magnetic phase transition are revealed.

The electronic structure calculations are performed using the full-potential nonorthogonal local-orbital minimum-basis band-structure scheme (FPLO) and employing the coherent potential approximation (CPA) to simulate disorder in a random way.[8] The FPLO-CPA method has been already employed by the authors to study the case of quaternary[9] and quinternary[10] half-metallic full-Heusler alloys and its results were in agreement with the ones provided earlier by the well-established Korringa-Kohn-Rostoker (KKR)-CPA method.[11] We have used the theoretical equilibrium lattice constants 5.73 Å for CoMnSb, 5.83 Å for NiMnSb, and 5.99 Å for CuMnSb, while the experimental ones are 5.87, 5.93, and 6.09 Å, respectively.[2] For the intermediate concentrations, we have assumed linear variation of the lattice constants. We should also note here that contrary to NiMnSb and CuMnSb, the perfect CoMnSb alloy does not crystallize in the $C1_b$ structure of semi-Heusler alloys but shows a more complex magnetic and lattice structure. This latter structure has been well understood using *ab initio* calculations in Ref. 12 as an alternation of Co_2MnSb and MnSb structural units. However, around the phase transition, which is of interest for us, the $Co_{1-x}Cu_xMnSb$ alloy crystallizes in the $C1_b$ structure assumed in our calculations.[4]

II. RESULTS AND DISCUSSION

The electronic and magnetic structure of the end compounds, i.e., CoMnSb, NiMnSb and CuMnSb has been extensively studied earlier and the reader is referred to Refs. 7 and 13 and the references therein for a detailed overview.

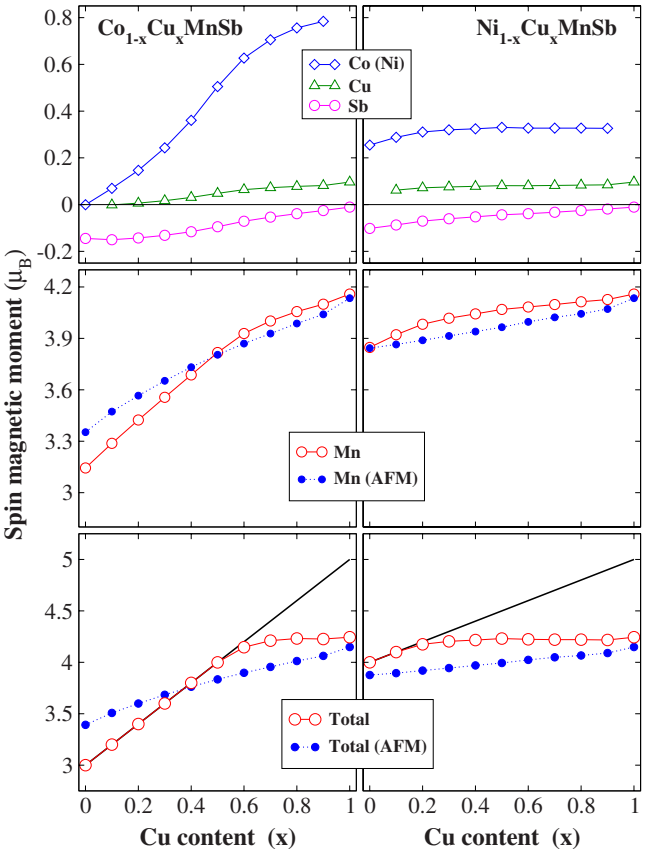

FIG. 1. (Color online) Calculated atom-resolved and total spin moments (in μ_B) in $Co_{1-x}Cu_xMnSb$ and $Ni_{1-x}Cu_xMnSb$ as a function of the Cu concentration (x). The atom-resolved spin moments for Co(Ni) and Cu have been scaled to one atom. Solid lines represent the Slater-Pauling rule. In the AFM case we provide the total spin moments per primitive unit cell since the total magnetization is zero.

Here we focus on the effect of the Cu doping on the magnetic characteristics of CoMnSb and NiMnSb, and we discuss the origin of the observed magnetic phase transition on the basis of the Anderson *s-d* mixing model. The discussion is divided into two parts. First, we study the influence of the Cu doping on the half-metallic gap; and second, we focus on the origin of the magnetic phase transition upon Cu doping including also a discussion on the role played by the magnetic reference state in interpreting the exchange mechanisms.

A. Effect of Cu doping on half-metallicity of CoMnSb and NiMnSb

In Fig. 1 we present the atom-resolved and total magnetic moments in $Co_{1-x}Cu_xMnSb$ and $Ni_{1-x}Cu_xMnSb$ as a function of the Cu content for the ferromagnetic state. For comparison the Mn magnetic moment corresponding to the antiferromagnetic state is given. Note that in the antiferromagnetic (AFM) state, the magnetic moments of Co(Ni) and Cu are zero for symmetry reasons, while Sb has a very small magnetic moment ($0.01-0.03\mu_B$) As seen from Fig. 1, for $x=0$ the corresponding parent compounds are half-metallic with total integer magnetic moments of $3\mu_B$ and $4\mu_B$ for CoMnSb and NiMnSb, respectively. As the Cu concentration increases, the total spin magnetic moment follows the Slater-Pauling rule up to $x \simeq 0.6$ ($x \simeq 0.2$) for the Co-based (Ni-based) system and then it becomes almost constant. Thus the half-metallicity is retained up to these particular values of the Cu concentration. This can also be seen from the total density of states (DOS) shown in Fig. 2, where the Fermi level cross the spin minority states for the corresponding values of x. Furthermore, the variation of the total magnetic moment is around $1.25\mu_B$ in the Co-based systems, which mainly comes from the Mn and Co atoms, whereas this is rather small ($\simeq 0.25\mu_B$) in the Ni-based systems. The behavior of the induced moments in Cu and Sb atoms only weakly depends on the x concentration. It should be noted that as seen from Fig. 1, the Mn moment is insensitive to the magnetic order revealing the localized nature of magnetism in half-metallic (HM) semi-Heusler alloys. It is important to note that similarity of the Mn magnetic moments in two different states is the consequence of the similarity of the Mn DOS, as shown in Fig. 3 for CuMnSb. These features justify the use of the Anderson *s-d* model in the interpretation of the results obtained from first principles.[15] Finally, we should note that the abrupt change in the magnetic moment in $Ni_{1-x}Cu_xMnSb$ observed in experiments for $x>0.8$ (Ref. 5) might be due to short-range correlations which are not captured by CPA calculations and thus it is not present in our results.

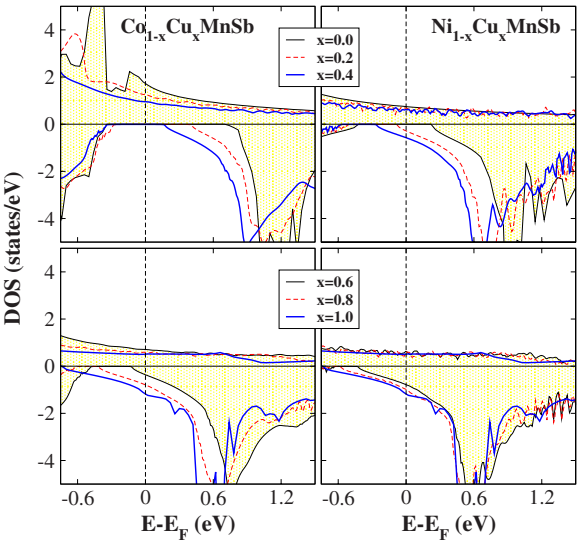

FIG. 2. (Color online) Spin-resolved total density of states (DOS) of $Co_{1-x}Cu_xMnSb$ and $Ni_{1-x}Cu_xMnSb$ around the Fermi level for selected values of x. Vertical dotted lines denote the Fermi level. Positive values of DOS correspond to the majority-spin electrons and negative values to the minority-spin electrons.

B. Origin of magnetic phase transition

In order to understand the origin of the experimentally observed magnetic phase transition, we calculate the total energies corresponding to the ferromagnetic (FM) and the AFM configurations of the Mn magnetic moments. We have used for all energy calculations the large AFM unit cell. The

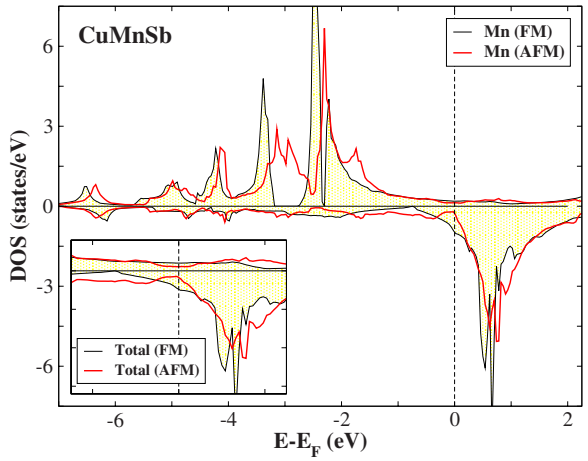

FIG. 3. (Color online) Spin-resolved Mn density of states of CuMnSb for FM and AFM configurations of the Mn magnetic moments. In the inset we show the total DOS around Fermi level. Broadening of the bands in AFM state might be due to strong hybridization with Cu and Sb atoms since large exchange splitting of the Mn 3*d* states prevents mixing of the spin-up and spin-down states of the Mn atoms at different sublattices. Note that in AFM state the local atomic spin-up states of one sublattice and local atomic spin-down states of other sublattice have the same projection on the global spin-quantization axis and can hybridize with each other (Ref. 14).

zero-temperature magnetic phase diagram is determined as the difference of the corresponding total energies ($E_{\mathrm{AFM}} - E_{\mathrm{FM}}$) per AFM unit cell and is presented in Fig. 4. In agreement with the experiments for both compounds, we obtain a phase transition from a ferromagnetic state to an antiferromagnetic one at a certain value of the Cu concentration x. As seen from Fig. 4 the critical x value for the Ni-based alloys

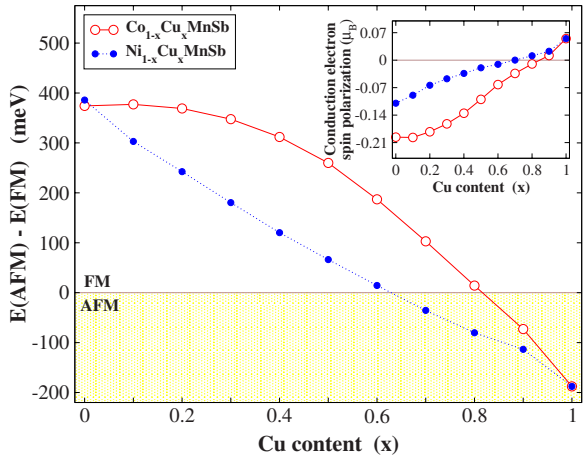

FIG. 4. (Color online) Ground-state magnetic phase diagram and total energy differences between AFM and FM configurations of the Mn magnetic moments in $Co_{1-x}Cu_xMnSb$ and $Ni_{1-x}Cu_xMnSb$ as a function of the Cu concentration (x). In the inset we show the total spin polarization of the conduction electrons of X (Co, Ni, Cu) and Z (Sb) atoms as a function of the Cu content. Note that the energy differences are given for an antiferromagnetic unit cell, while spin polarization of the conduction electrons is given for a FM unit cell.

($x \simeq 0.6$) is somehow smaller than the experimental value ($0.9 < x < 1$), while in the Co-based compounds the transition point ($x \simeq 0.8$) is closer to the measured value ($0.9 < x < 1$). The smaller concentration for the phase transition predicted by theory is probably due to the smaller lattice parameters used in the calculations since compression of the lattice shifts the Fermi level to higher energies, increasing consequently the weight of the AFM superexchange contribution. The HM character, as discussed above, is lost before reaching the transition point and the Fermi level crosses the minority-spin conduction band but the ferromagnetism persists up to the transition point. Finally, for CuMnSb our calculated energy difference is ~200 meV, while in Ref. 7 it is around 50 meV. The difference may be due to different orientations of Mn magnetic moments ([001] in the present work and [111] in Ref. 7) and the smaller lattice parameter used in the present work (5.99 Å instead of 6.09 Å).

As shown in Ref. 16 the observed magnetic phase transition in these systems can be qualitatively accounted for in terms of the competition of the ferromagnetic Ruderman-Kittel-Kasuya-Yosida (RKKY)-type exchange and antiferromagnetic superexchange. Note that a detailed discussion of the exchange mechanism in local-moment systems and applications to different systems can be found in Refs. 17 and 18. Here we will give the expressions for both exchange couplings in the $\mathbf{q} \to 0$ limit for the analysis of the obtained results. For $\mathbf{q}=0$ the RKKY-type coupling takes a simple form, which is $J_{\mathrm{RKKY}}(0) = V^4 D(\epsilon_F)/E_h^2$, where V is the coupling between the Mn 3*d* levels and the conduction-electron states. The mixing interaction V induces a spin polarization in the conduction-electron sea, and the propagation of this polarization gives rise to an effective indirect exchange coupling between distant magnetic moments. $D(\epsilon_F)$ is the density of states at the Fermi level and E_h is the energy required to promote an electron from the occupied 3*d* levels to the Fermi level. It is worth noting that the parameter E_h is not well defined for the present systems because of the broadening of the Mn 3*d* levels into the energy bands crossing the Fermi level. Thus the only parameter which can be used to estimate the relative contribution of the ferromagnetic RKKY-type coupling is the spin polarization of the conduction electrons. On the other hand, the superexchange coupling does not possess a simple limit; for $\mathbf{q}=0$ it becomes $J_S(0) = V^4 \Sigma_{nk} [\epsilon_F - \epsilon_{nk} - E_h]^{-3}$, where the sum is taken over the unoccupied states and the terms in this sum drop off quickly as ϵ_{nk} increases. Thus, the structure of the DOS above the Fermi level plays a key role in determining the strength of this coupling. We should finally note that we have not extracted from our calculations the exchange constants and consequently the Curie temperature since (i) methods such as frozen-magnon approximation for calculation of former quantities is not implemented in FPLO and (ii) we cannot use alternatively the energy differences in Fig. 4 due to the long-range character of the interactions. This latter approach can be used for systems having short-range (nearest-neighbor) exchange coupling.

Now we return to the discussion of the phase diagram in terms of these two mechanisms. Qualitative information on the variation of the RKKY-type and superexchange contributions can be obtained from the analysis of the conduction-

electron spin polarization and from the structure of the DOS above the Fermi level. As seen in Figs. 2 and 4 when we substitute Cu for Co(Ni), the spin polarization decreases and at the same time the position of the Fermi level moves toward higher energies; i.e., the number of the states just above the Fermi level increases. This gives rise to an opposite behavior in the relative contributions of the exchange mechanisms: a decrease in the RKKY-type coupling and an increase in the superexchange mechanism. In the large part of the phase diagram, the former coupling dominates. This is reflected as a correlation between the spin polarization and the total energy differences given in Fig. 4. On the other hand, the superexchange coupling becomes important for larger values of the Cu concentration, i.e., for $x>0.5$. As seen from Fig. 4 at the transition points both mechanisms compensate for each other, giving rise to a spin-glass-like behavior.[19] Further increase in x leads to an antiferromagnetic order in both compounds due to the dominating character of the superexchange mechanism. On the other hand, the sign of the calculated spin polarization is an important quantity in classifying the present systems and revealing the coupling mechanism between conduction electrons and local moment. Note that this coupling stems from two distinct processes: electrostatic Coulomb exchange and *sp-d* mixing interaction. The former mechanism induces a net positive spin polarization, while the contribution of latter is always negative and disappears in strong magnetic limit.[20] As seen from Fig. 4 up to the phase transition points, both systems possess negative spin polarization, i.e., *sp-d* mixing is dominating. At the magnetic phase transition point, spin polarization changes sign; and afterward in a very small region, it becomes positive. This behavior shows that up to the very large Cu concentrations, both systems can be characterized as weak ferromagnets.

As discussed above the magnetic interactions in HM semi-Heusler alloys are sensitive to the width of the gap and the position of the Fermi level within the gap. Systems that have large HM gaps and a Fermi level far from the right edge of the gap are strongly ferromagnetic and possess very high Curie temperatures.[21–25] This is due to the fact that in this case the superexchange mechanism is less efficient since the gap in the spin-down channel decreases the number of available minority-spin states just above the Fermi level. Thus, the position of the Fermi level within the gap is an important parameter in determining the magnetic characteristics of the HM ferromagnets. These findings suggest a way for tuning the magnetic properties of the HM ferromagnets and allow the fabrication of materials with predefined characteristics. It should be noted that, as shown in Ref. 16, the variation in the *sp*-electron (Z atom) concentration is an alternative route for tuning the magnetic properties of the Heusler alloys. However, in HM compounds both kind of atoms give rise to similar effects, as demonstrated by recent experiments.[3,5]

Finally, we would like to comment on the discussion of exchange mechanisms with respect to different reference state. So far we consider only FM state as a reference state for interpretation of the first-principles calculations. However, for ideal local-moment systems any reference state (FM or AFM) can be used for calculation of exchange constants. Sandratskii *et al.*[26] gave a detailed analysis of the issue considering AFM Fe monolayer on top of W(001). Using frozen-magnon technique, the authors demonstrated that the study of the instability of the ferromagnetic state predicts the ground-state antiferromagnetic structure. However, the exchange constants calculated for FM and AFM reference states appeared to be quite different and this discrepancy was attributed to the limitations of the Heisenberg model in the description of the magnetism in the Fe/W(001) system. Since in Mn-based Heusler alloys the Mn magnetic moments are well localized compared to other 3*d* intermetallics,[27,28] one expects a different situation for the exchange interactions; i.e., any reference state yields similar pattern of exchange parameters. However, consideration of the AFM state as a reference state does not provide a clear picture for the interpretation of the exchange mechanisms. Although the Mn DOS in transition from FM to AFM state remains qualitatively the same (see Fig. 3), the spin polarization of the conduction electrons vanishes due to symmetry properties. Thus, AFM reference state does not seem to be appropriate for a qualitative interpretation of the exchange mechanisms in Heusler alloys within the Anderson *s-d* mixing model.

III. CONCLUSIONS

In conclusion, we study the effect of the nonmagnetic 3*d* atoms on the magnetic properties of the half-metallic Mn-based semi-Heusler alloys $Co_{1-x}Cu_xMnSb$ and $Ni_{1-x}Cu_xMnSb$ $(0\leq x\leq 1)$ within the framework of the parameter-free density-functional theory. We show that the magnetic interactions in these systems strongly depend on the position of the Fermi level within the gap. We show that for Cu concentrations preserving the half-metallic character, the ferromagnetic RKKY-type exchange mechanism dominates, while the antiferromagnetic superexchange coupling becomes important for larger Cu concentrations and it is responsible for the observed magnetic phase transition in both compounds. These findings can be used as a practical tool to design materials with given physical properties.

*galanakis@upatras.gr
†e.sasioglu@fz-juelich.de
‡kozdogan@gyte.edu.tr

[1] I. Galanakis, P. H. Dederichs, and N. Papanikolaou, Phys. Rev. B **66**, 174429 (2002).
[2] P. J. Webster and K. R. A. Ziebeck, in *Alloys and Compounds of d-Elements with Main Group Elements, Part 2*, edited by H. R. J. Wijn, Landolt-Börnstein, New Series, Group III, Vol. 19, Pt. C (Springer-Verlag, Berlin, 1988).
[3] C. Walle, L. Offernes, and A. Kjekshus, J. Alloys Compd. **349**, 105 (2003).
[4] N. P. Duong, L. T. Hung, T. D. Hien, N. P. Thuy, N. T. Trung,

and E. Brück, J. Magn. Magn. Mater. **311**, 605 (2007).
[5] S. K. Ren, W. Q. Zou, J. Gao, X. L. Jiang, F. M. Zhang, and Y. W. Du, J. Magn. Magn. Mater. **288**, 276 (2005).
[6] J. Bœuf, C. Pfleiderer, and A. Faiszt, Phys. Rev. B **74**, 024428 (2006).
[7] T. Jeong, R. Weht, and W. E. Pickett, Phys. Rev. B **71**, 184103 (2005).
[8] K. Koepernik and H. Eschrig, Phys. Rev. B **59**, 1743 (1999); K. Koepernik, B. Velicky, R. Hayn, and H. Eschrig, *ibid.* **58**, 6944 (1998).
[9] K. Özdoğan, B. Aktaş, I. Galanakis, and E. Şaşıoğlu, J. Appl. Phys. **101**, 073910 (2007).
[10] K. Özdoğan, E. Şaşıoğlu, and I. Galanakis, J. Appl. Phys. **103**, 023503 (2008).
[11] I. Galanakis, J. Phys.: Condens. Matter **16**, 3089 (2004).
[12] V. Ksenofontov, G. Melnyk, M. Wojcik, S. Wurmehl, K. Kroth, S. Reiman, P. Blaha, and C. Felser, Phys. Rev. B **74**, 134426 (2006).
[13] E. Şaşıoğlu, L. M. Sandratskii, P. Bruno, and I. Galanakis, Phys. Rev. B **72**, 184415 (2005).
[14] L. M. Sandratskii, Adv. Phys. **47**, 91 (1998).
[15] P. W. Anderson, Phys. Rev. **124**, 41 (1961).
[16] E. Şaşıoğlu, L. M. Sandratskii, and P. Bruno Appl. Phys. Lett. **89**, 222508 (2006); Phys. Rev. B **77**, 064417 (2008).
[17] C. E. T. Gonçalves Da Silva and L. M. Falicov, J. Phys. C **5**, 63 (1972).
[18] Z.-P. Shi, P. M. Levy, and J. L. Fry, Phys. Rev. B **49**, 15159 (1994).
[19] P. Ferriani, I. Turek, S. Heinze, G. Bihlmayer, and S. Blügel, Phys. Rev. Lett. **99**, 187203 (2007).
[20] R. E. Watson, S. Koide, M. Peter, and A. J. Freeman, Phys. Rev. **139**, A167 (1965); R. E. Watson, A. J. Freeman, and S. Koide, *ibid.* **186**, 625 (1969).
[21] J. Kübler, Phys. Rev. B **67**, 220403(R) (2003).
[22] A. Sakuma, J. Phys. Soc. Jpn. **71**, 2534 (2002).
[23] B. Sanyal, L. Bergqvist, and O. Eriksson, Phys. Rev. B **68**, 054417 (2003).
[24] J. Rusz, L. Bergqvist, J. Kudrnovský, and I. Turek, Phys. Rev. B **73**, 214412 (2006).
[25] E. Şaşıoğlu, I. Galanakis, L. M. Sandratskii, and P. Bruno, J. Phys.: Condens. Matter **17**, 3915 (2005).
[26] L. M. Sandratskii, E. Şaşıoğlu, and P. Bruno, Phys. Rev. B **73**, 014430 (2006).
[27] S. Plogmann, T. Schlatholter, J. Braun, M. Neumann, Y. M. Yarmoshenko, M. Yablonskikh, E. I. Shreder, E. Z. Kurmaev, A. Wrona, and A. Slebarski, Phys. Rev. B **60**, 6428 (1999).
[28] J. Kübler, A. R. Williams, and C. B. Sommers, Phys. Rev. B **28**, 1745 (1983).